International Journal of Electrical, Electronic and Communication Sciences
ISSN: 2517-9438
Vol:10, No:7, 2016

# Characterization of Inertial Confinement Fusion Targets Based on Transmission Holographic Mach-Zehnder Interferometer

B. Zare-Farsani, M. Valieghbal, M. Tarkashvand, A. H. Farahbod

***Abstract*****—**To provide the conditions for nuclear fusion by high energy and powerful laser beams, it is required to have a high degree of symmetry and surface uniformity of the spherical capsules to reduce the Rayleigh-Taylor hydrodynamic instabilities. In this paper, we have used the digital microscopic holography based on Mach-Zehnder interferometer to study the quality of targets for inertial fusion. The interferometric pattern of the target has been registered by a CCD camera and analyzed by Holovision software. The uniformity of the surface and shell thickness are investigated and measured in reconstructed image. We measured shell thickness in different zone where obtained non uniformity 22.82 percent.

***Keywords*****—**Inertial confinement fusion, Mach-Zehnder interferometer, Digital holographic microscopy.

## I. Introduction

ONE common technique known that leads to energy production is inertial confinement fusion (ICF). In inertial confinement fusion, uniform compression of the target depends on the target structure, as well as the intensity and shape, of the driving pulse. Fabrication of targets for inertial fusion is critical to ensure that the bombarding laser energy yields high compression of the target. To minimize Rayleigh–Taylor instabilities, current direct drive ICF targets require specific surface finishes. Homogeneity of the thickness and sphericity has to be realized. In addition, density variations and nonspherical or nonconcentric shells produced during the fabrication process can cause hydrodynamic instabilities. The nonuniformities are the dominant source of perturbations, which cause a departure from one-dimensional performance.

ICF aims at achieving fusion by compressing the fusion fuel to high densities albeit for a short period of time. In the ICF process, a tiny sphere (known as the capsule or pellet), is filled with a mixture of two isotopes of hydrogen (deuterium (D) and tritium (T)) and is subjected to a sudden application of intense pressure and high temperature. The pressure is provided either directly by the light of laser, by the conversion of laser light into x-rays, or by an x-ray generating device such as a Z-pinch machine. This pressure forces rapid heating and a subsequent ablation of some of the material of the outer layer of the capsule. In many respects, this process is similar to the process by which the Sun produces its energy, though the Sun system uses gravitational confinement [1], [2]. Polymer shells having a good fuel retention capability are desirable in inertial confinement fusion experiments. The primary interest in a polymer shell is based on the low average atomic number which suppresses the growth of hydrodynamic instability during implosion. The polymers, however, generally have low fuel retention capability and are easily degraded by beta decay of tritium. In order to perform ICF experiments, the polymer shell must have good barrier properties and resistance to beta radiation. Polystyrene is one of the materials used in ICF capsules [3]. In this regard, the geometric characterization of target, such as external surface imperfections, nonspherical or nonconcentric shells, homogeneity of the thickness is considered important part in the project inertial confinement fusion. Thus, characterization and quality control ICF targets at each stage of production play main role in preparing blast temperature and density needed to fuel nuclear heat. There are a number of methods for diagnosing elemental uniformity and concentrations in materials. Typical ICF targets are spheres less than a millimeter in diameter. Optical methods are cost-effective for characterization of laser fusion targets and these produced high quality images. Digital holography takes the basics of classical holography concerning whole 3-D information (complex amplitude distribution) of the object wavefront but with the advantages of digital processing methods provided by computers [4], [5]. First evidences of image formation with digitally reconstructed holograms were reported more than 50 years ago. Nowadays, electronic image recording devices (typically a CCD or a CMOS camera) have replaced holographic recording media. Thus, digital holography arises from the same holographic principles than classical holography but replacing the recording medium and a complete parallelism can be established between classical and digital holography. Digital holography is combined with microscopy to avoid the high magnification ratios needed in conventional optical microscope imaging. Moreover, digital holographic microscopy (DHM) allows 3-D sample imaging by numerical reconstructing of a two-dimensional (2-D) image. Due to its interferometric underlying principle, different classical interferometric configurations can be used to assemble a DHM setup [6]-[10]. In that sense, Mach-Zehnder [11], Michelson [26], Twyman-Green [27], and common-path [28] interferometric architectures have been proposed as basis layouts. Among them, Mach-Zehnder configuration is by far the most used one in DHM practice [11]-[25]. Mach-Zehnder configuration is the selected setup used in the experimental implementation included along this

B. Zare-Farsani, M. Valieghbal, M. Tarkashvand and A. H. Farahbod are with the School of Plasma Physics and Nuclear Fusion, NSTRI, Tehran-Iran (e-mail: zarefarsani@gmail.com).

paper. Resolution interferometric measurement is a fraction of (100 nm) the laser wavelength where Characterization of target outer surface with high quality is possible [29]-[31].

The Fresnel or Fourier holograms are recorded directly by the CCD and stored digitally. No film material involving wet-chemical or other processing is necessary. The reconstruction of the wavefield, which is done optically by illumination of a hologram, is performed by numerical methods. The numerical reconstruction process is based on the Fresnel–Kirchhoff integral, which describes the diffraction of the reconstructing wave at the micro-structure of the hologram. In the numerical reconstruction process not only the intensity, but also the phase distribution of the stored wavefield can be computed from the digital hologram.

The holographic process is described mathematically as:

$$O(x,y) = o(x,y)\exp(i\varphi_0(x,y)) \quad (1)$$

is the complex amplitude of the object wave with real amplitude o and phase $\varphi_0$ and

$$R(x,y) = r(x,y)\exp(i\varphi_R(x,y)) \quad (2)$$

is the complex amplitude of the reference wave with real amplitude r and phase $\varphi_R$. Both waves interfere at the surface of the recording medium. The intensity is calculated by

$$I(x,y) = |O(x,y) + R(x,y)|^2 = (O(x,y) + R(x,y))(O(x,y) + R(x,y))^* = R(x,y)R^*(x,y) + O(x,y)O^*(x,y) + O(x,y)R^*(x,y) + R(x,y)O^*(x,y) \quad (3)$$

where * denotes the conjugate complex. The amplitude transmission h(x,y) of the developed photographic plate (or any other recording media) is proportional to I(x,y):

$$h(x,y) = h_0 + \beta\tau I(x,y) \quad (4)$$

where β is a constant, τ is the exposure time and $h_0$ is the amplitude transmission of the unexposed plate. h(x,y) is also called the hologram function. In digital holography, using CCDs as recording medium $h_0$ can be neglected.

For hologram reconstruction, the amplitude transmission has to be multiplied with the complex amplitude of the reconstruction (reference) wave:

$$R(x,y)h(x,y) = [h_0 + \beta\tau(r^2 + o^2)]R(x,y + \beta\tau r^2 O(x,y) + \beta\tau R^2(x,y)O^*(x,y). \quad (5)$$

The first term on the right side of this equation is the reference wave, multiplied by a factor. It represents the undiffracted wave passing through the hologram (zero diffraction order).

The second term is the reconstructed object wave, forming the virtual image. The factor $\beta\tau r^2$ only influences the brightness of the image. The third term produces a distorted real image of the object. For off-axis holography the virtual image, the real image and the undiffracted wave are spatially separated. In optical reconstruction, the virtual image appears at the position of the original object and the real image is formed also at a distanced, but in the opposite direction from the CCD. The diffraction of a light wave at an aperture (in this case a hologram) which is fastened perpendicular to the incoming beam is described by the Fresnel–Kirchhoff integral:

$$\Gamma(\xi,\eta) = \frac{i}{\lambda}\int_{-\infty}^{\infty}\int_{-\infty}^{\infty} h(x,y)R(x,y)\frac{\exp(-i\frac{2\pi}{\lambda}\rho)}{\rho} \times (\frac{1}{2} + \frac{1}{2}cos\theta)dxdy \quad (6)$$

with

$$\rho = \sqrt{(x-\xi)^2 + (y-\eta)^2 + d^2} \quad (7)$$

where h(x,y) is again the hologram function and ρ is the distance between a point in the hologram plane and a point in the reconstruction plane. For a plane reference wave R(x,y) is simply given by the real amplitude:

$$R = r + i0 = r \quad (8)$$

The diffraction pattern is calculated at a distance d behind the CCD plane, which means it reconstructs the complex amplitude in the plane of the real image.

Equation (6) is the basis for numerical hologram reconstruction. Because the reconstructed wave field $\Gamma(\xi,\eta)$ is a complex function, both the intensity as well as the phase can be calculated [32]. This is in contrast to the case of optical hologram reconstruction, in which only the intensity is made visible.

## II. Experimental

### A. Method of Sample Preparation

Polystyrene microballon are made Microencapsulation method at School of Plasma Physics and Nuclear Fusion, NSTRI, Tehran-Iran. We have used microencapsulation method to prepare PS hollow microspheres as polymer targets. In this method, W/O (water in oil) emulsion is first formed in which water globules are dispersed in polystyrene solution. This is followed by a W/O/W emulsion in which shells of polystyrene solution containing water are dispersed in polyvinyl alcohol solution in water.

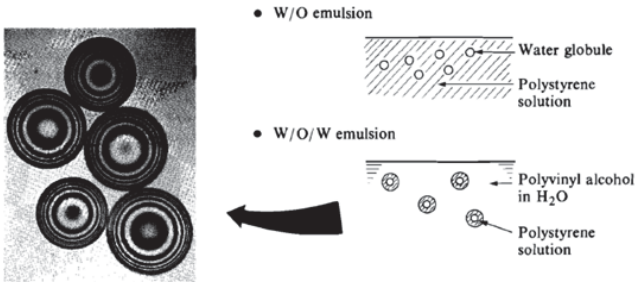


Fig. 1 Schematic of microencapsulation technique of forming plastic shells

Approximately target diameter is 100-400 $\mu m$ that its structure is shown in Fig. 2. To carry out measurements, the targets had to be mounted securely. This was achieved by

mounting individual targets onto the tips of glass capillary using a suitable adhesive (gluewater). The mounted targets were held in a vertical orientation on top of glass capillary. Befor target irradiated, target image had recorded by CCD's microscope (1280×1024 HV, 3mega pixels) in order to ensure its flawless. Microscopic image of a mounted target is shown in Fig. 3.

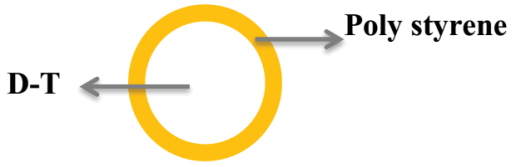


Fig. 2 Schematic of laser fusion targets

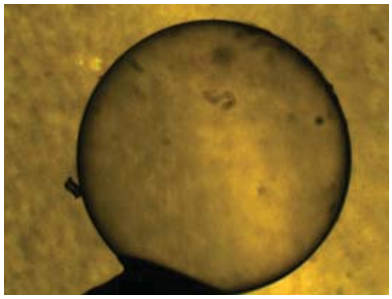

Fig. 3 Microscopic image of laser fusion targets

*B. Experimental Setup*

The experimental setup assembled at the laboratory is the same one depicted in Fig. 4 where a He-Ne laser source is used as illumination wavelength. The object is placed d=0.18 m from the CCD array of 1280×960 pixels with pixel size Δx=Δy=4.67μm. The wavelength is 632.8 nm. Light coming from a laser is split by a first beam splitter (BS1) allowing the implementation of a Mach-Zehnder architecture. On one branch (the imaging branch), we place a microscope setup in transmission mode. The microscope objective produces a magnified image of the transparent sample. On the other branch, the light incoming from BS1 is expanded and collimated giving rise to the reference beam. After reflection in the tilted bending mirror and in the beam splitter BS2, the reference beam impinges on the CCD. The tilt in the bending reference mirror allows the reference beam to reach the CCD at oblique incidence, forming a small angle θ with the propagation direction of the object beam.

A typical digital hologram is shown in Fig. 5. Recorded hologram has been reconstructed by Holovision software (Fresnel method) and the background has been removed by MVS and HPF filters. Final reconstructed image is shown in Fig. 6. Shell thickness cannot be determined at the microscopic image whereas it can be determined at reconstructed image. Therefore, the DHM method is superior to microscopic imaging. Shell thickness was measured in different parts of the reconstructed image because the target thickness uniformity is important. Measured values and the percentage of non-uniform thickness are given in Table I.

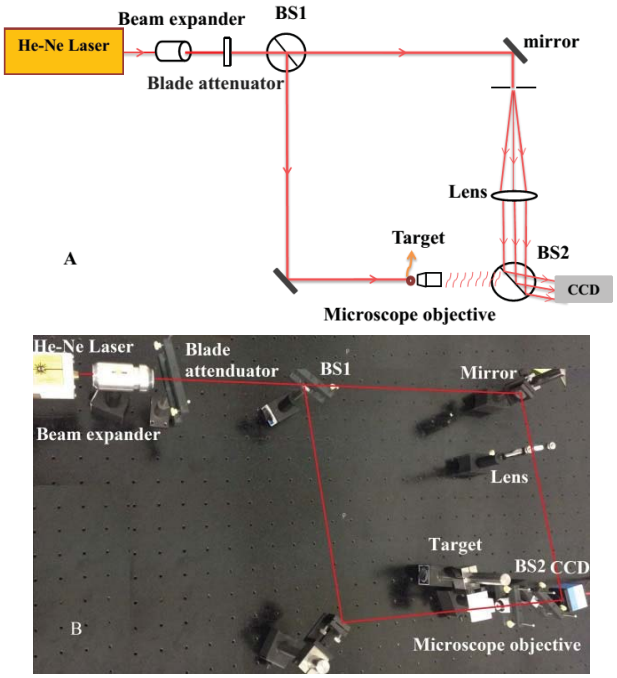


Fig. 4 (A) Optical setup of Match-Zehnder interferometric configuration in a DHM. (B) Pictures of the experimental setup at the laboratory

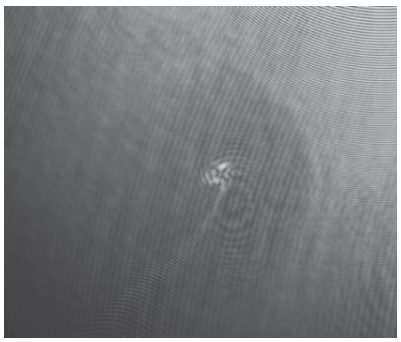

Fig. 5 Interference pattern of target

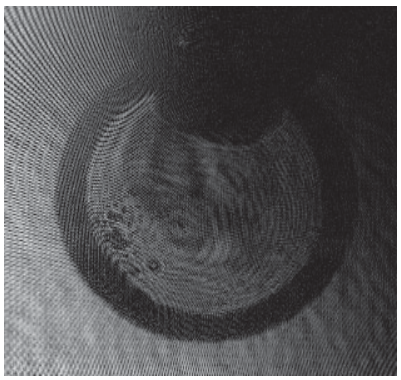

Fig. 6 Reconstructed image

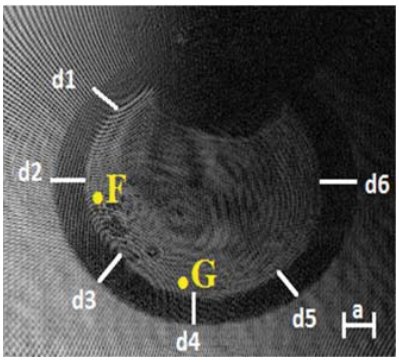


Fig. 7 Shell thickness in d1, d2, d3, d4, d5, d6 in term of "a" scale (a = 18 μm) and Homogeneous target from F to G

TABLE I
SHELL THICKNESS AT SIX POSITION IDENTIFIED IN FIG. 7

| position | Shell thickness (a = 18 μm) | Percent of Non-uniformity Shell |
|---|---|---|
| **d1** | 1.13a | 13% |
| **d2** | 1.39a | 39% |
| **d3** | 1.21a | 21% |
| **d4** | 0.96a | -4% |
| **d5** | 1.23a | 23% |
| **d6** | 1.45a | 45% |

The results show approximately 22.83 percent of non-uniformity shell at different position. In addition, Intensity profile is plotted in term of position to examine the homogeneity of the space inside the shell. Intensity profile is plotted in term of position from F (77,125) to G (145,180) by holovision software (distance between there equaled 87.45 μm) shown in Fig. 8. Intensity variations in different areas proved heterogeneity of the labeled position.

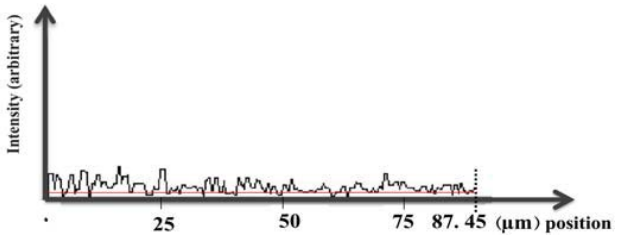


Fig. 8 Intensity in term of position from F to G

## III. CONCLUSION

Targets for laser fusion should have high degree of sphericity, surface uniformity, and homogeneity. So choose the appropriate method for quality control capsules made is very important. In this paper, digital microscopic holography based on Mach-Zehnder interferometer is used. The hologram of the target has been recorded by a CCD camera and reconstructed by Holovision software. Measurements show approximately 22.83 percent of non-uniformity shell at different position in reconstructed image. The uniformity of the surface and shell thickness are investigated and measured in reconstructed image. We measured shell thickness in different zone where obtained non uniformity 22.82 percent. Also Intensity variations (Intensity profile is not coincide on red constant line) in different areas proved heterogeneity.

## REFERENCES

[1] B.Kursunoglu, A. Perlmutter, S. M. Widmayer, "Progress in lasers and laser fusion" sprringer (1975).
[2] John F. Holzrichter, Ph.D, "Lasers and inertial fusion experiments at livermore" Lawrence Livermore Laboratory Report (2006).
[3] L. A. Scott, R. G. Schneggenburger, and P. R. Anderson, J. Vac. Sci. Technol. A4, 1155 (1986).
[4] T. P. Bernat, D. H. Darling, and J. J. Sanchez, "Applications of holographic interferometry to cryogenic ICF target characterization" Lawrence Livermore Laboratory Report (1982).
[5] L. P. Yaroslavsky, Digital Holography and Digital Image Processing: Principles, Methods, Algorithms (Kluwer, 2003).
[6] L. Yu and M.K. Kim, "Wavelength-scanning digital interference holography for tomographic 3D imaging using the angular spectrum method," Opt. Lett. 30, 2092-2094 (2005).
[7] Goodman JW, Lawrence RW. Digital image formation from electronically detected holograms. Appl. Phys. Lett. 1967; 11: 77-79.
[8] Huang T. Digital holography. Proc. IEEE. 1971; 59: 1335-1346.
[9] Schnars U, Jüpter WPO. Digital Holography. Springer-Verlag, Heidelberg; (2005).
[10] Yaroslavsky LP. Digital Holography and Digital Image Processing: Principles, Methods, Algorithms. Kluwer Academic Publishers, Massachusetts; (2003).
[11] Zhang T, Yamaguchi I. Three-dimensional microscopy with phase-shifting digital holography. Opt. Lett.(1998); 23: 1221-1223
[12] Cuche E, Marquet P, Depeursinge C. Simultaneous amplitude-contrast and quantitative phase-contrast microscopy by numerical reconstruction of Fresnel off-axis holograms. Appl. Opt. (1999); 38: 6994-7001.
[13] Dubois F, Joannes L, Legros JC. Improved three-dimensional imaging with a digital holography microscope with a source of partial spatial coherence. Appl. Opt. (1999); 38: 7085-7094.
[14] Colomb T, Dürr F, Cuche E, Marquet P, Limberger HG, Salathé RP, Depeursinge C. Polarization microscopy by use of digital holography: application to optical-fiber birefringence measurements. Appl. Opt.2005; 44: 4461-4469.
[15] Colomb T, Kühn J, Charrière F, Depeursinge C, Marquet P, Aspert N. Total aberrations compensation in digital holographic microscopy with a reference conjugated hologram. Opt. Express 2006; 14: 4300-4306.
[16] Ferraro P, Grilli S, Alfieri D, De Nicola S, Finizio A, Pierattini G, Javidi B, Coppola G, Striano V. Extended focused image in microscopy by digital holography. Opt. Express2005; 13: 6738-6749.
[17] Ferraro P, Coppola G, De Nicola S, Finizio A, Pierattini G. Digital holographic microscope with automatic focus tracking by detecting sample displacement in real time. Opt. Lett.2003; 28: 1257-1259.
[18] Marquet P, Rappaz B, Magistretti PJ, Cuche E, Emery Y, Colomb T, Depeursinge C. Digital holographic microscopy: a noninvasive contrast imaging technique allowing quantitative visualization of living cells with subwavelength axial accuracy. Opt. Lett.2005; 30: 468-470.
[19] Dubois F, Minetti C, Monnom O, Yourassowsky C, Legros JC, Kischel P. Pattern recognition with a digital holographic microscope working in partially coherent illumination. Appl. Opt.2002; 41: 4108-4119.
[20] Charrière F, Kühn J, Colomb T, Montfort F, Cuche E, Emery Y, Weible K, Marquet P, Depeursinge C. Characterization of microlenses by digital holographic microscopy. Appl. Opt.2006; 45: 829-835.
[21] Coppola G, Ferraro P, Iodice M, De Nicola S, Finizio A, Grilli S. A digital holographic microscope for complete characterization of microelectromechanical systems. Meas. Sci. Technol.2004; 15: 529-539.
[22] Rappaz B, Marquet P, Cuche E, Emery Y, Depeursinge C, Magistretti P. Measurement of the integral refractive index and dynamic cell morphometry of living cells with digital holographic microscopy. Opt. Express2005; 13: 9361-9373.
[23] Kemper B, von Bally G. Digital holographic microscopy for live cell applications and technical inspection. Appl. Opt.2008; 47: A52-A61.
[24] Shi H, Fu Y, Quan C, Tay CJ, He X. Vibration measurement of a micro-structure by digital holographic microscopy. Meas. Sci. Technol.2009; 20: 065301.
[25] Wahba HH, Kreis T. Characterization of graded index optical fibers by digital holographic interferometry. Appl. Opt.2009; 48: 1573-1582.

[26] Iwai H, Fang-Yen C, Popescu G, Wax A, Badizadegan K, Dasari RR, Feld MS. Quantitative phase imaging using actively stabilized phase-shifting low-coherence interferometry. Opt. Lett.2004; 29: 2399-2401.
[27] Reichelt S, Zappe H. Combined Twyman-Green and Mach-Zehnder interferometer for microlens testing. Appl. Opt.2005; 44: 5786-5792.
[28] Mico V, Zalevsky Z, Garcia J. Common-path phase-shifting digital holographic microscopy: A way to quantitative phase imaging and superresolution. Opt. Commun.2008; 281: 4273-4281.
[29] Micó V, Ferreira C, Zalevsky Z and García J. Superresolution digital holographic microscopy for three-dimensional samples. (2008).
[30] Micó V, Ferreira C, Zalevsky Z and García J. Basic principles and applications of digital holographic microscopy. (2010).
[31] Uichi K, Hitoshi N, and Hyo-gun K. Fabrication of cross-linked polymer shells for inertial confinement fusion experiments. (1997).
[32] Schnars U. Direct phase determination in hologram interferometry with use of digitally recorded holograms. (1994).